An Emerging Coherent Picture of Red Supergiant Explosions

Dovi Poznanski[1*]

[1]School of Physics and Astronomy, Tel-Aviv University, Tel Aviv 69978, Israel.

[*]To whom correspondence should be addressed; E-mail: dovi@tau.ac.il.

A large fraction of supernovae (SNe) arise from the core collapse of red supergiant stars. By comparing the ejecta velocities of a large sample of such SNe with initial stellar masses derived from pre-explosion images of the progenitor star, I find that there is a significant and approximately linear relation between initial mass and ejecta velocity, which in turn implies that the energy released during core collapse and captured by the ejecta depends strongly on this mass as $\mathrm{E} \propto \mathrm{M}^3$. This correlation naturally explains why most such SNe have almost identical "plateau-phase" durations in their light curves, and places an important constraint on the elusive physics of core collapse.

Type II supernovae (SNe) are the most common type of stellar explosion (*1*), and have long been known to arise from the core collapse of massive stars. They exhibit prominent lines of hydrogen in their spectra, indicative of a massive envelope of unprocessed material, and they are typically found near regions of star formation. Numerous progenitor stars have been identified in archival images, taken before the SN exploded (*2*). In the most secure cases, post-mortem images have shown that the presumed progenitor has indeed disappeared. The majority of these SNe, called Type II-P, have optical light curves that are well described by a fast rise (up to a few days), a long "plateau-phase" that is mostly powered by a reprocessing of the energy deposited

by the shock into radiation, followed by a sharp decline, and then an exponential decline that is fueled by the radioactive decay of newly formed ^{56}Co. Their progenitors are red supergiants.

As the star collapses its core rebounds, and a shock wave ensues. A small fraction of the energy of the shock, of order one percent, suffices to expel the envelope of the star, leaving a compact remnant (a neutron star or a black hole). Analytical and numerical studies predict relations between the intrinsic and observed properties, but they seem at odds with several robust observations. However, if the kinetic energy of the ejecta is proportional to the mass cubed, then theory and observations agree, and there is strong evidence detailed below that this is indeed the case.

I compile from the literature a comprehensive set of initial stellar masses (or mass limits) of 23 Type II-P SNe (*3–10*). In order to probe the energy deposited in the ejecta, for 17 of these SNe, I derive ejecta velocity by measuring the blueshift of the minimum of the FeII $\lambda 5169$ absorption feature using over 100 spectra (SOM §2). These velocities are translated to velocities at day 50 past explosion using the same algorithm used for the standardized candle method (*11*).

Figure 1 shows the velocities and masses for the sample. Assuming a monotonic relation between initial mass and ejecta mass, and a roughly constant energy, E, deposited by the explosion, one would expect that velocity, v, will decline with increasing mass. This is simply a consequence of $\mathrm{E} \propto \mathrm{M v}^2/2$, as the thermal energy supplied by the shock is converted into two components, a kinetic one that expels the envelope, and a radiative component that provides the optical luminosity of the SN. However, the figure shows that the opposite is true. There are no high-mass progenitors with low-velocity ejecta, and while there is a significant correlation, its slope is positive. A Pearson test returns a correlation significance of 98 percent. This correlation extends from the lowest-mass sub-luminous class up to SN 2009kr, which is at the extreme of the II-P range, possibly outside of it (SOM §1.1).

Since there are substantial uncertainties on both axes, and no preferred 'dependent' or 'independent' variable, I perform a bisector least square fit to a power-law of the form $\mathrm{M}[\mathrm{M}_\odot] \propto \mathrm{v}^{\mathrm{a}}[10^3 \mathrm{km\,s}^{-1}]$ on bootstrapped data (*12*). When using only SNe with determined masses I find a best fit $a = 1 \pm 0.1$. When I include also the mass limits the fit tends towards a slightly shallower dependence, with $a = 0.9 \pm 0.1$, although this is likely an underestimate of the power-law index (SOM §3). An orthogonal least-squares fit similarly gives a power-law dependence with index of order unity. There is no compelling evidence that any SN is an outlier. Rejecting one or another SN, including SN 2009kr, which may seem to drive the correlation at high masses, does not alter the result. All objects are within 2σ of the best fit relation, and a slope of zero is inconsistent with the data at the 6σ level.

I consequently find that the velocity of the ejecta during the plateau phase correlate approximately linearly with the initial mass, such that $\mathrm{M} \propto \mathrm{v}$. Various analytical models have calculated the dependence of the observable SN luminosity and timescale, L and $\mathrm{t_p}$, on the kinetic energy, ejecta mass, and initial radius, E, $\mathrm{M_{ej}}$, and $\mathrm{R_*}$, respectively. Assuming a diffusion-dominated evolution (*13*), one dominated by the effect of hydrogen recombination (*14, 15*), or a more complex combination of both (*16*), somewhat different scalings have been predicted.

A common feature of these various models is that, while they differ on the assumed physics, they arrive at an identical relative contribution of the mass and the energy to the luminosity and the timescale, regardless of the details. Generally speaking, they find that

$$\mathrm{t_p} \propto \mathrm{E}^{-\alpha}\, \mathrm{M_{ej}}^{3\alpha}\, \mathrm{R_*}^{\beta}. \tag{1}$$

The parameters α and β depend on the model, but are usually close to $0.15 - 0.2$ (β is zero for the diffusion model).

With no obvious a-priori relation between the intrinsic parameters that will cancel out their contribution, it is hard to reconcile this equation with observational evidence that plateau du-

rations have a narrow distribution (*11, 17*). However, assuming that the initial stellar mass is roughly proportional to the mass ejected during the explosion (SOM §4), I replace $\mathrm{M_{ej}}$ with M, the kinetic energy $\mathrm{E} \propto \mathrm{M\,v^2} \propto \mathrm{M^3}$. Substituting for E or M in Equation (*1*), the dependences on energy and mass cancel out, and $\mathrm{t_P}$ depends only on the radius to a small power (or not at all, depending on the model). A variation of nearly a factor of 2 in radii will translate at most to a 15% variation in plateau length, which is consistent with observations (I do neglect the late time contribution to the light curve of ^{56}Ni decay). Radii measured for many of the progenitors in this sample seem to broadly agree with this picture (*3*). Therefore, the finding that $\mathrm{E} \propto \mathrm{M^3}$ can be deduced from the fact that plateau lengths (and radii) have narrow ranges.

Hydrodynamical and radiative transfer simulations recover results which are consistent with equation (*1*) (*18, 19*). Furthermore, using a recently calculated extensive grid of models (*20*), where the authors vary the kinetic energy and mass independently, I extract the plateau length at every mass that obeys the constraint that $\mathrm{M} \propto \mathrm{v}$. As can be seen in Figure (2), the large range of timescales that these models span is dramatically reduced once this requirement is introduced. Additionally, I find that the plateau length is somewhat anti-correlated with mass and energy, such that higher-mass models have shorter plateaus. This is a prediction that should be tested with future data, and is consistent with the current picture in which the highest mass Type II SNe do not have a plateau at all, having lost most of their envelope via winds (SOM §4).

The scaling law for the luminosity can be similarly expressed as

$$\mathrm{L} \propto \mathrm{E}^{\gamma}\,\mathrm{M_{ej}}^{\frac{2-\gamma}{3}}\,\mathrm{R_*}^{\delta}, \tag{2}$$

where the different models predict quite different values for γ and δ. Substituting v for E and M in Equation *2* one gets $\mathrm{L} \propto \mathrm{v}^2\,\mathrm{R}_*^{\delta}$. This is in agreement with the empirical finding that the luminosity of Type II-P SNe correlate with photospheric velocity (*11, 21, 22*), as long as the dependence on the radius is weak, as predicted by some of the models.

There is an even simpler and less model-dependent way to look at the luminosity, as it is roughly the available energy internal to the radius of the emitting object over time. Replacing the energy with the energy remaining after adiabatic losses,

$$\mathrm{L} \propto \frac{\mathrm{E_{int}(R)}}{\mathrm{t}} \propto \mathrm{E}\,\frac{\mathrm{R_*}}{\mathrm{R(t)\,t}}. \tag{3}$$

Further replacing $\mathrm{R(t)}$ with vt, and E with $\mathrm{Mv^2}$ the luminosity simply scales as

$$\mathrm{L} \propto \frac{\mathrm{MvR_*}}{\mathrm{t^2}}, \tag{4}$$

where t is the typical timescale, which can be replaced with $\mathrm{t_p}$. A constant plateau length and $\mathrm{M} \propto \mathrm{v}$ therefore imply that $\mathrm{L} \propto \mathrm{v^2 R_*}$, and variations in radius and plateau length may partially cancel out, reducing the scatter.

The findings of this work can be summarized as follows. The approximately linear relation between mass and velocity of Type II-P SNe implies a strong dependence of the explosion energy on the initial mass, of order $\mathrm{E} \propto \mathrm{M^3}$. This ties in together analytical and numerical models that have predicted a wide range of possible plateau lengths, with the observation of a small range of durations. In addition, the scatter in duration is likely due to differences in progenitor radii. Ongoing surveys that are probing the SN evolution during the first few days past explosion can constrain the radius at the time of explosion (*23, 24*), and thus test this prediction. Additionally, these findings are naturally consistent with the known relation between luminosity and velocity.

The implications of the puzzling result that the energy of SN explosions depends strongly on the progenitor mass are beyond the scope of this paper. Nevertheless, it is likely an important clue regarding the mechanism that couples the large energy released during core collapse to the ejected mass, and leading to a successful explosion. A factor of about 2.5 in progenitor mass ($\sim 8 - 20\,\mathrm{M_\odot}$) translates into a factor of 15 in energy. The most natural place to allow for such a variation is not in the total available energy (which would naively depend only on the

core), but in the efficiency of the deposition process, be it via neutrinos, instabilities, or any other mechanism summoned to successfully explode the star. If the energy deposition process is slow (*25*), the binding energy of the envelope has an important impact on the energetics of its subsequent expulsion.

References and Notes

1. W. Li, *et al.*, *MNRAS* **412**, 1441 (2011).
2. S. J. Smartt, *ARA&A* **47**, 63 (2009).
3. S. J. Smartt, J. J. Eldridge, R. M. Crockett, J. R. Maund, *MNRAS* **395**, 1409 (2009).
4. M. Fraser, *et al.*, *MNRAS* **417**, 1417 (2011).
5. R. M. Crockett, *et al.*, *MNRAS* **410**, 2767 (2011).
6. J. Maund, E. Reilly, S. Mattila, *ArXiv: 1302.7152* (2013).
7. S. D. Van Dyk, *et al.*, *ApJ* **756**, 131 (2012).
8. M. Fraser, *et al.*, *ApJL* **759**, L13 (2012).
9. A. Jerkstrand, *et al.*, *A&A* **546**, A28 (2012).
10. J. R. Maund, *et al.*, *MNRAS* **431**, L102 (2013).
11. D. Poznanski, *et al.*, *ApJ* **694**, 1067 (2009).
12. G. J. Babu, E. D. Feigelson, *Communications in Statistics-Simulation and Computation* **21**, 533 (1992).
13. W. D. Arnett, *ApJ* **237**, 541 (1980).

14. S. E. Woosley, *ApJ* **330**, 218 (1988).

15. N. N. Chugai, *Soviet Astronomy Letters* **17**, 210 (1991).

16. D. V. Popov, *ApJ* **414**, 712 (1993).

17. I. Arcavi, *et al.*, *ApJL* **756**, L30 (2012).

18. I. Y. Litvinova, D. K. Nadezhin, *Soviet Astronomy Letters* **11**, 145 (1985).

19. D. Kasen, S. E. Woosley, *ApJ* **703**, 2205 (2009).

20. L. Dessart, E. Livne, R. Waldman, *MNRAS* **408**, 827 (2010).

21. M. Hamuy, P. A. Pinto, *ApJ* **566**, L63 (2002).

22. P. Nugent, *et al.*, *ApJ* **645**, 841 (2006).

23. A. Gal-Yam, *et al.*, *ApJ* **736**, 159 (2011).

24. I. Sagiv, *et al.*, *ArXiv: 1303.6194* (2013).

25. L. Dessart, E. Livne, R. Waldman, *MNRAS* **405**, 2113 (2010).

26. First and foremost, I am grateful to my friends and colleagues who have systematically gathered the large body of observations that I have used here. I am no less thankful to A. Gal-Yam, R. Helled, I. Kleiser, A. Levinson, E. Livne, D. Maoz, E. Nakar, H. Netzer, B. Trakhtenbrot, and S. Van Dyk, for valuable advice regarding many aspects of this work. I am further indebted to A. Filippenko for allowing me access to his impressive database of SN data. S. Benetti and the Padova SN group are thanked for the spectrum of SN 2004dg. M Stritzinger, G. Pignata, and the Carnegie SN program are thanked for the spectra of SN 2008bk. A. Gal-Yam and the Palomar Transient Factory are thanked

for the spectra of SN 2012aw. The PESSTO collaboration is thanked for the spectra of SN 2012ec. This work made use of the Weizmann interactive supernova data repository (www.weizmann.ac.il/astrophysics/wiserep), as well as the NASA/IPAC Extragalactic Database (NED) which is operated by the Jet Propulsion Laboratory, California Institute of Technology, under contract with the National Aeronautics and Space Administration. I further acknowledge the support of the Alon fellowship for outstanding young researchers, and from the Raymond and Beverly Sackler chair for young scientists.

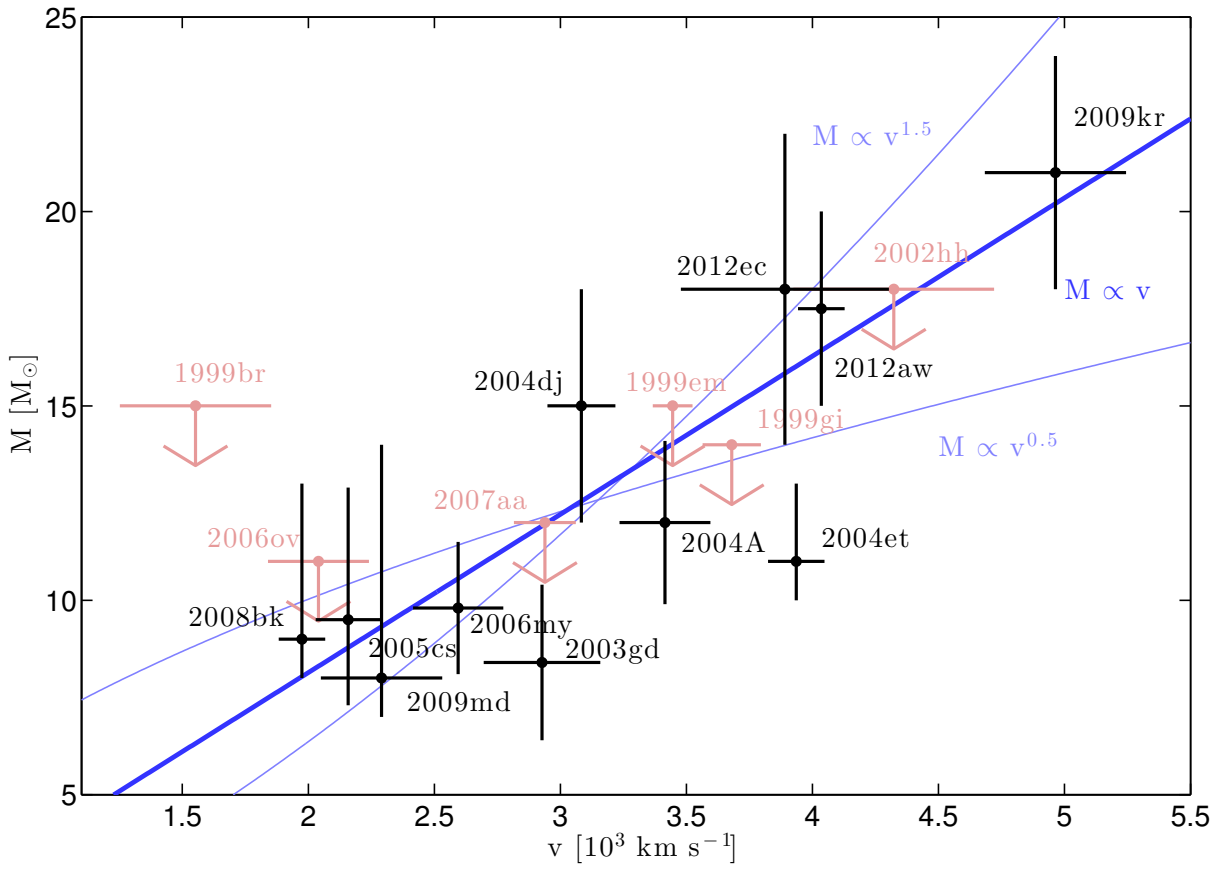

Fig. 1. Black crosses show the ejecta velocities and initial stellar masses for a sample of Type II-P SNe with progenitors detected in pre-explosion images. Objects with only upper limits on the mass appear as pink arrows. Data are consistent with a linear trend between velocity and mass, as can be seen with the best fit power law in dark blue. For comparison, steeper and shallower (inconsistent) dependences are plotted in light blue.

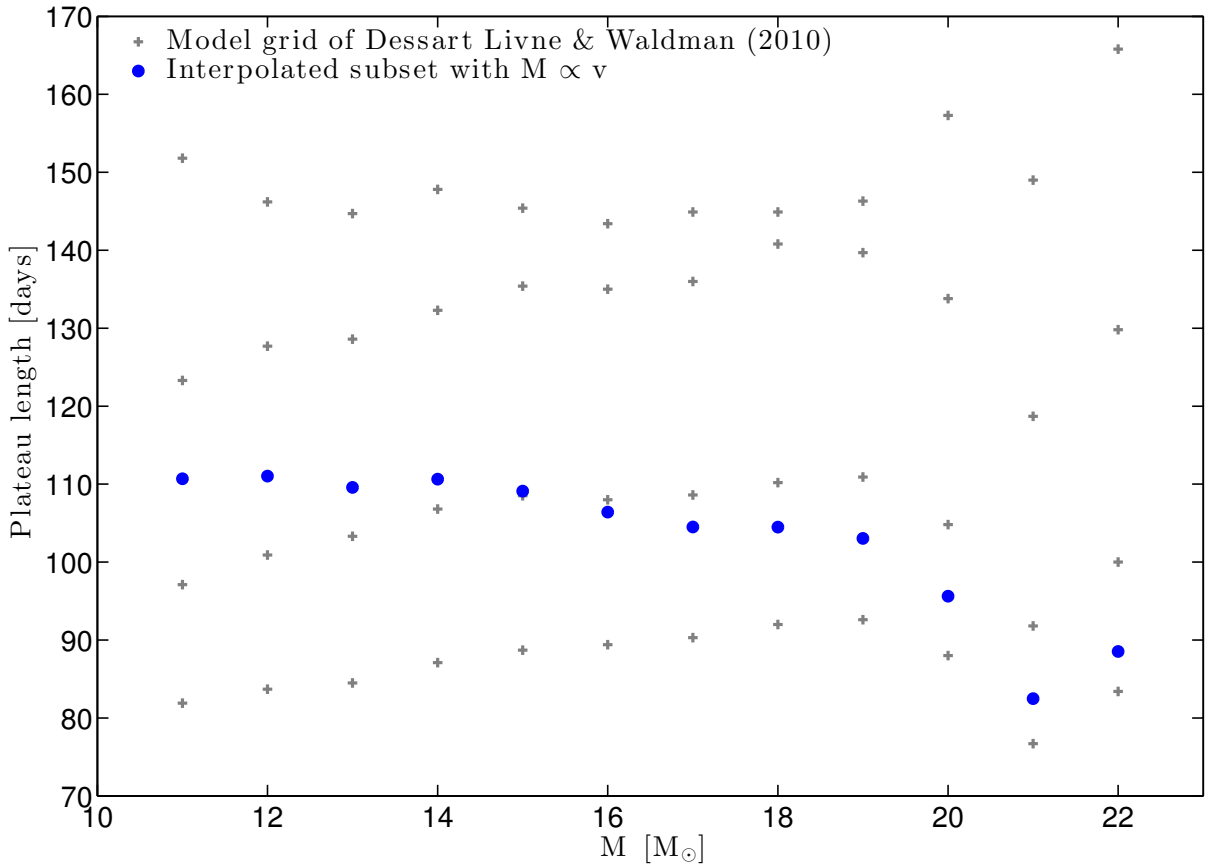

Fig. 2. Masses and plateau lengths for a grid of models (*20*) in grey crosses, and for the subset that follows $\mathrm{M} \propto \mathrm{v}$ in blue dots. The wide range of a-priori possible timescales is substantially reduced as predicted from observations and the scaling relations. Furthermore these results predict a slight decrease in duration with mass.

Supporting Online Material

1 Progenitor Sample

The focus of this study is SNe II-P. (*1*) and later (*2*) compiled a comprehensive list of progenitor mass determinations, including a self consistent re-derivation of some of the masses. (*3*) revisit three of these masses, (*4*) revisit five more, and I further add SNe 2009kr (*5, 6*), and the recently discovered 2012aw (*7, 8*) and 2012ec (*9*). In table S1 I list the masses as compiled from these sources.

Determining the mass of these progenitors depends on an array of modeling tools and assumptions, most notably regarding the dust that enshrouds them, the distances to their host galaxies, and the details of their pre-SN evolution. These difficulties are unavoidable in attempting to link a handful of observed colors and brightnesses, measured a cosmic moment before explosion at a post main-sequence stage, to initial conditions set millions of years before. This entails large statistical uncertainties, and equally substantial systematic ones. As this field progresses, methods improve, further observations are obtained after the SN has faded, and some determinations are revised.

(*4*) find that the previously identified progenitor of SN 1999ev is actually still present in images taken after the SN has faded. They discuss various possibilities. First, the unresolved source may be a cluster that is now one star short. Second, the source may be unrelated. Last, the new source might be a light echo, and the progenitor has indeed disappeared. The authors find the probability for the last two options to be rather low, and they therefore discard the previously measured mass for this progenitor.

I find a very low velocity for this SN of about $2200\,\mathrm{km\,s^{-1}}$, which would make a $16\,\mathrm{M_\odot}$ progenitor a significant outlier to the mass-velocity relation. The low velocity reinforces the findings of (*4*) and point to a low mass progenitor, near $8\,\mathrm{M_\odot}$. This example indicates that the mass-velocity relation can help us differentiate between progenitor candidates in ambiguous

cases.

The progenitor mass of SN 2004et is difficult to measure, since it is based on ground based data and requires non-trivial subtraction of neighboring stars that are contaminating the photometry. The $8\,M_{\odot}$ mass derived by (*3*) is being revised by Fraser et al. (in prep) as quoted by (*10*). The new higher mass of $11\,M_{\odot}$ is also consistent with competing efforts (Van Dyk, private communication). For this reason I use the higher mass for SN 2004et as quoted in (*10*). For this SN as well, the correlation here can be seen as an indication that the lower mass estimate was indeed erroneous, though it is only 2σ away from the best fitting relation.

There is some risk in including SN 2009kr in my analysis. As discussed below it is not a 'classical' II-P and may actually come from a different progenitor channel. There is also some controversy regarding its mass. While (*5*) advocate a $21\,M_{\odot}$, which we use, (*6*) argue for a mass near $15\,M_{\odot}$, claiming that the comparison to stellar tracks that have not finished core helium burning is misguided. Without favoring one or other analysis, I do note that the progenitor is consistent with recent stellar tracks for $20\,M_{\odot}$ stars that include the effects of pulsation-driven superwinds (*11*). The luminosity and temperature measured for the progenitor are in perfect agreement with their pre-SN predictions. In practice, either mass would be consistent with a linear mass-velocity relation, and in light of the most recent result of (*11*), I keep the higher mass, with caution. An alternative way of looking at this debate would be to infer that a higher mass is slightly more probable, as it is more consistent with the mass-velocity relation as derived from the rest of the sample.

1.1 Supernovae II-L

The historic division between Type II-P and II-L SNe is photometric, and is based on the observation that some Type II SNe do not show a pronounced plateau (*12, 13*). However this segregation is based on observations in blue colors, where most SNe show some decline, and predates the spectroscopic discovery and definition of type IIn and IIb SNe that indeed often

show a somewhat linearly declining light curve. The first are mostly powered by interaction with the circumstellar medium, and can therefore have wildly different light curves depending on the mass-loss history. The latter are intermediate between Type I and Type II and are interpreted as being transition objects with a thin hydrogen shell, visible in early spectra until the photosphere moves more deeply in. Their photometric evolution is therefore more similar to the ^{56}Ni powered Type Ib/c SNe.

SN 1979C, and SN 1980K are often referred to as the prototypical II-L SNe, but in the same breath are called 'over luminous' and 'peculiar' (*14*). When studying the cosmological utility of SNe II-P it has been noted that some of the otherwise normal looking SNe which show a rather subtle decline in I-band photometry, are outliers on the Hubble diagram (*15*). This has led some to classify objects that decline by about 1 mag over the ~ 100 day plateau as II-L (*16*).

Recently, studying a sample of R-band light curves (*17*) have found that indeed there is a subsample of Type II SNe that decline by about that much, and that they do not form a continuum with the normal plateau objects. Studies of the spectroscopic features of these SNe are still preliminary (*18*). At least from a photometric perspective SN 2009kr seems to belong to this class. Whether or not these indeed form a distinct class of SNe, in terms of their photometric and spectroscopic, as well as intrinsic properties, is still a mostly open question.

2 Spectroscopy

It has been strongly established that the luminosity of Type II-P SNe correlates with the photospheric velocity during the plateau phase, as traced by the Fe II lines (*19*). The correlation of the ejecta velocities of SNe II-P – as measured from the blueshift of the FeII $\lambda 5169$ absorption feature – with their luminosities makes these SNe promising 'standardizeable candles' (*15, 20, 21*). This is further supported by numerical efforts showing that indeed this line traces the photosphere reasonably well (*22*) and obtaining the luminosity-velocity correlation using a grid of

models (*23*).

I compile spectra taken during the plateau phase using publicly available resources (*24*), supplemented mostly by spectra obtained by the group of A. Filippenko at UC Berkeley (*25*). Using the SNID code (*26*), every spectrum is cross-correlated with a set of high signal-to-noise spectra with manually measured velocities. The resulting velocities are then propagated to day 50 using the power law $v(50) = v(t)(t/50)^{0.464\pm0.017}$ (*20*) and averaged using their uncertainties as weights. I keep only objects for which the resulting velocity uncertainty is smaller than $1000\,\mathrm{km\,s^{-1}}$.

Since SNe II-P evolve slowly during the plateau phase, both spectroscopically and photometrically, their properties in the middle of the plateau are less sensitive to systematics arising from uncertainties regarding the precise explosion date. As the velocity approximately declines like $t^{-0.5}$ (*20*), an uncertainty of ±10 days implies a velocity uncertainty of only ±10 percent.

Still, there can be a significant uncertainty for some SNe that were discovered late. In order not to bias velocity measurements, I do not use spectroscopic information for phase determination, relying instead on photometric constraints alone. For most SNe the explosion date is conservatively set as the midpoint between discovery and last non-detection with an uncertainty that spans that time range. For some objects, where such a constraint is weak and overestimates the uncertainty, I use the end of the plateau phase as an indicator that 100 ± 10 days have passed since explosion. Table S2 summarizes the spectroscopic data.

3 Velocity vs. Mass – Detailed Statistical Analysis

It has been noted that sub-luminous SNe II-P tend to have determined progenitor masses at the low end of possible masses, i.e., near $8\,\mathrm{M_\odot}$ (*2*). While it might make sense from a simplistic argument of energetics that smaller masses will produce underwhelming explosions, it is unclear whether there is indeed a correlation between mass and luminosity that extends beyond the

lower-mass regime. A major hurdle is that SN luminosities are difficult to measure. Most importantly, the luminosity depends on the amount of dust and the distance that one measures or assumes.

As detailed in my main manuscript, there is substantial evidence for a correlation in Figure (1), based on a variety of statistical significance tests. However, with the large uncertainties in the masses, their non-gaussian uncertainties, and the non negligible uncertainties in velocity, standard out-of-the-box tools often used by astronomers will fail to give a reliable answer.

In order to make it a linear (and symmetric) fit, in the discussion below I take the logarithm of both velocity and mass, and subtract the mean from each variable. The slope of the best fit line is the best fit power.

There are multiple solutions in the literature for dealing with uncertainties on both variables, and a lack of straightforward definition of the dependent or independent variable (*27–29*). A simple example can elucidate the difficulty. If we were to fit a linear model to random uncorrelated x and y variables, a standard least square fit will find a best fit slope for $(y|x)$ of zero - parallel to the abscissa. However, inverting the variables and fitting for the slope of $(x|y)$, one would get zero as well, parallel to our previous ordinate. Of course neither are significant, but this example shows how when the scatter is large the choice of dependent or independent variable can dramatically change the result. One simple solution, called the bisector least-square method, is to take the line that bisects the two solutions presented above.

I use the bisector method, while bootstrapping the data, which allows me to sample the distribution of the slope recovered, and therefore its uncertainty. Using the sample of 17 SNe and limits I find a slope of 1 ± 0.1. The bootstrapping confirms that no single SN, (i.e., particularly not SN 2009kr) is driving the fit, since the bootstrap algorithm can pick any 17 objects, with repetition, at any of the hundreds of thousands of instances produced.

Another method, called the orthogonal least square method, is to measure orthogonal dis-

tances from the best fit line rather than vertical distances (i.e., along the y-axis). This creates the needed symmetry between the variables as well. This gives a consistent slope of 0.9 ± 0.1.

I perform a Pearson correlation test on $100,000$ bootstrapped samples, and obtain a correlation coefficient distribution which is centered on 0.55 ± 0.2. The same test on randomly permuted pairs returns 0.05 ± 0.2, with values higher than 0.55 for only 2 percent of the samples. Various other tests, correlation measures, resampling methods, all give a similar conclusion, that the correlation is significant and its slope of order unity.

In order to include also the mass limits and treat them as measurements, I must assume some prior distribution on their mass, as well as an upper error which is not commonly reported for limits (i.e., if an object has a limit of $\mathrm{M} < 10\,\mathrm{M}_{\odot}$ could the progenitor have with some probability a mass of $11\mathrm{M}_{\odot}$ or $10.1\mathrm{M}_{\odot}$?). If I assume upper errors that are a third of the typical error on mass for all the mass determinations (a crude approximation to the fact that non-detections are typically 3σ) and lower errors that reach to a minimum mass of $6\mathrm{M}_{\odot}$ it tends to pull the fit towards a slightly slower dependence, with $a = 0.8 \pm 0.1$. This is most likely an under estimate of the power, since by assuming 1σ error bars that reach $6\mathrm{M}_{\odot}$ I effectively imply that a large fraction of progenitors have masses smaller than that, which is contradictory to our understanding of stellar collapse.

One should also ask why many of the SNe with mass limits lie so close to the correlation. First, it should be noted that I did not attempt to collect or measure velocities for SNe with very weak progenitor mass limits (beyond the few I had available). I therefore do not have many objects with mass limits lying in the high-mass sector of the figure (though, as can be seen in the SOM, this would add 2 SNe at most). Second, from volumetric reasons most objects found by surveys are near the flux limit. If indeed there is a correlation between mass and velocity and between velocity and luminosity as discussed below, given a non-detection of the progenitor, the posterior mass probability of every SN is skewed towards higher mass. If there is no correlation

there should be no such preference, and the limits should not lie so close to the relation. Had there been no correlation one would have expected the limits to populate the parameter space much more randomly. The mass limits by themselves therefore suggest a correlation.

The best fit trend consistently has a χ^2 smaller than the number of degrees of freedom regardless of the subsample used, which is expected considering the large error bars. This also indicates that current data are unable to constrain the intrinsic scatter in the relation between mass and velocity.

4 Initial vs. Ejected Mass and Comparison to Numerical Models

There are various masses involved – the initial mass, the pre-explosion mass, the remnant mass, and the ejecta mass. In the main analysis I treat the initial and ejecta mass as practically interchangeable. The difference between the two masses are the mass of the stellar remnant, for which it is safe to assume a mass of order 1–2 $M_\odot$, and the effects of mass loss from stellar birth to demise. The latter process is poorly understood, but it is likely that for relatively small masses (i.e., 6 $M_\odot <$ M $< 15\,M_\odot$) there is a rather linear dependence of the mass loss on mass. At higher masses mass loss becomes more efficient and can effectively leave a smaller pre-SN star regardless of the initial mass. This picture is consistent with the models in Table 2 of (*23*).

Using this table as a prescription (see Figure 1) to transform the initial masses of the progenitors to ejected masses does not alter the picture in any significant way. The transformation is essentially linear for all but one SN (SN 2009kr) and does not introduce a significant change, within the existing mass uncertainties. Because this change does lower higher-mass objects more significantly, the best fit power-law, while still being consistent with a linear relation, is about 10% smaller for both analysis methods presented above.

A grid of models has been calculated (*30*) where the authors predominantly vary the mass

between 11 and 30 $M_\odot$ and the kinetic energy that is pumped into the ejecta, probing the range between 0.1 and 3 times 10^{51} erg. As shown in Figure (2) of the main manuscript, when applying the constraint $M \propto v$ the wide range of plateau lengths that the models predict are narrowed down to a very tight distribution. In addition, Figure (S2) shows that the energy values that follow this same constraint also correlate with mass, with a best fit power of $E \propto M^2$. This value is somewhat lower than found from observations, but could be understood as resulting from the conversion between initial and ejecta mass. As shown in Figure S3, replacing initial masses with ejecta masses from the models one recovers the $E \propto M^3$ relation. This however breaks down, as initial masses exceed 20 $M_\odot$, at which point mass loss can bring a more massive star to have smaller ejecta, linking the realm of II-P SNe to their more massive II-L cousins, of which SN 2009kr is possibly an example.

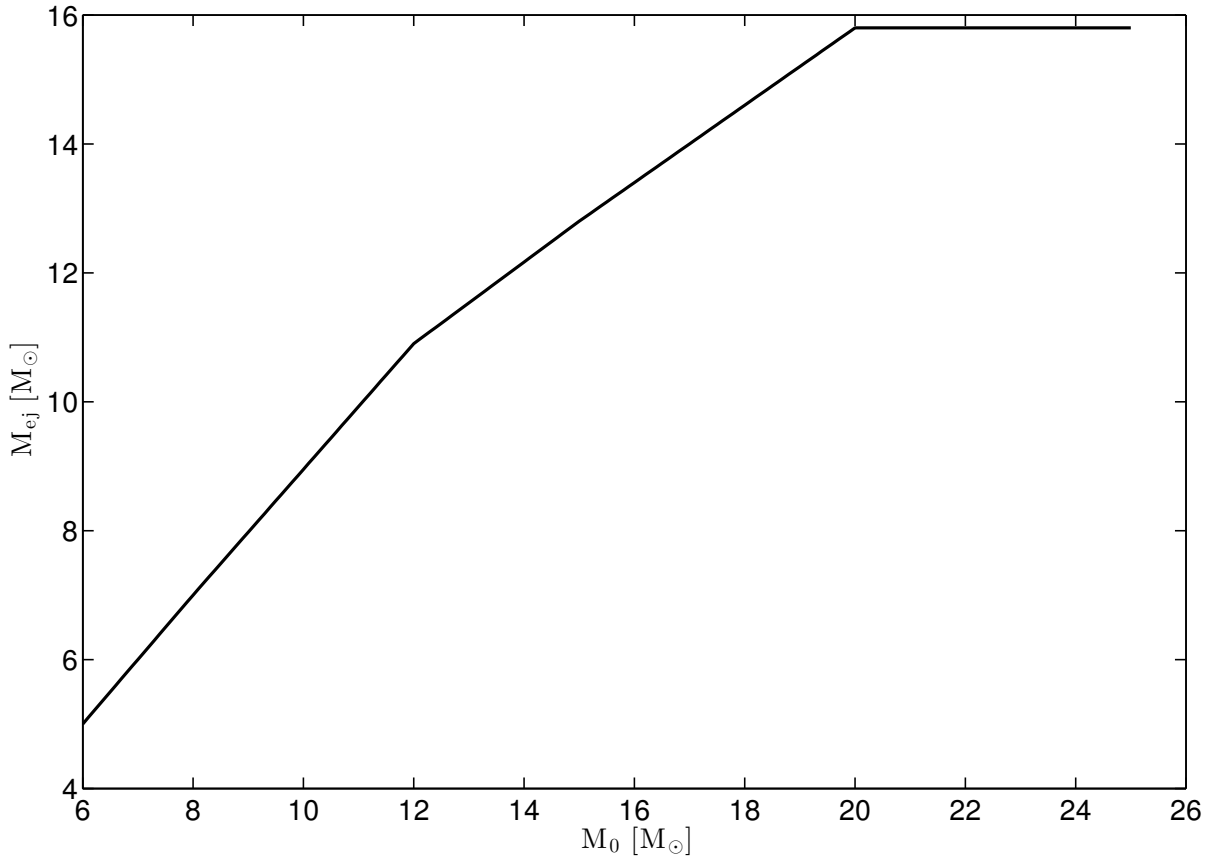

Fig. S1. Ejected mass vs. initial mass, interpolating the models in (*23*). Using these derived masses does not alter our conclusions, at most reducing the best fit power-law by about 10%.

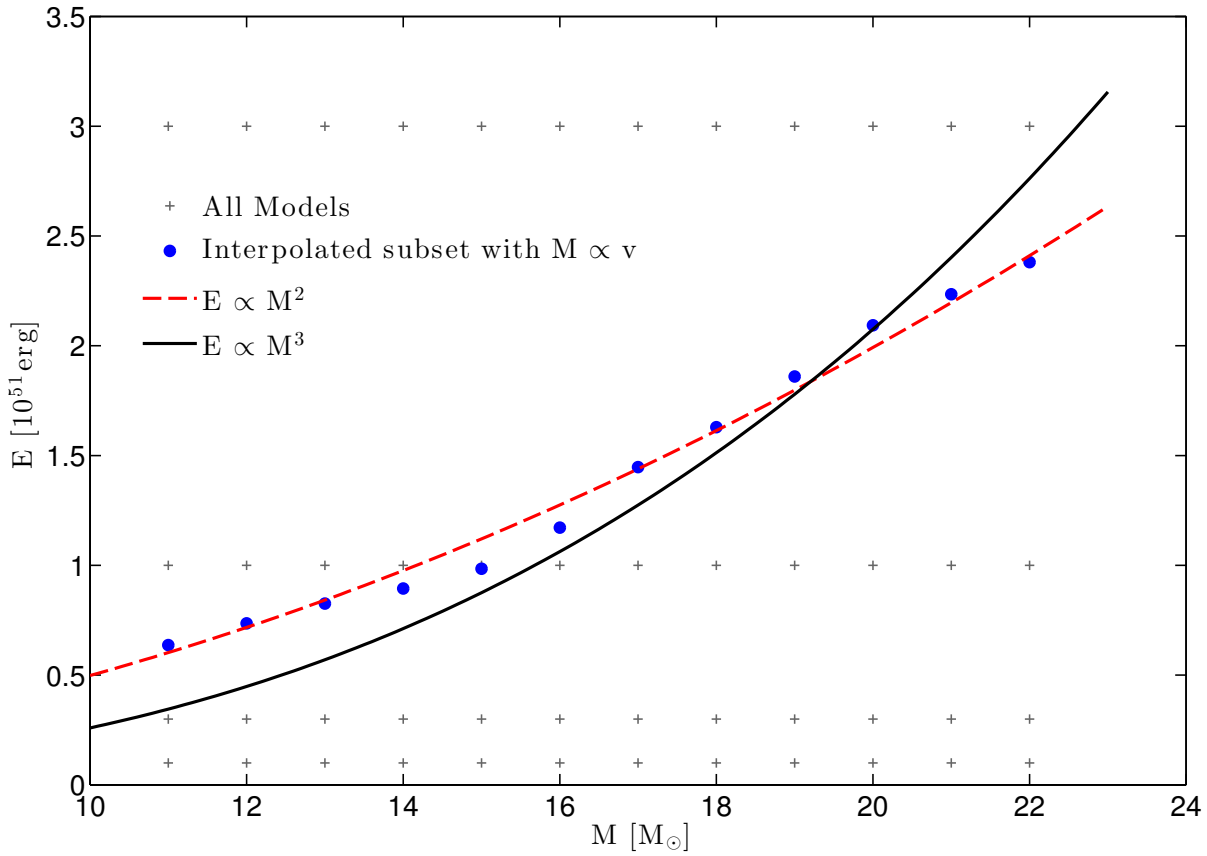

Fig. S2. Kinetic energy vs. initial mass, interpolating the models in (*30*) that obey $\mathrm{M} \propto \mathrm{v}$. This confirms the finding that energy rises with mass, albeit with a somewhat smaller power. See however text for a possible explanation, as well as Figure S3.

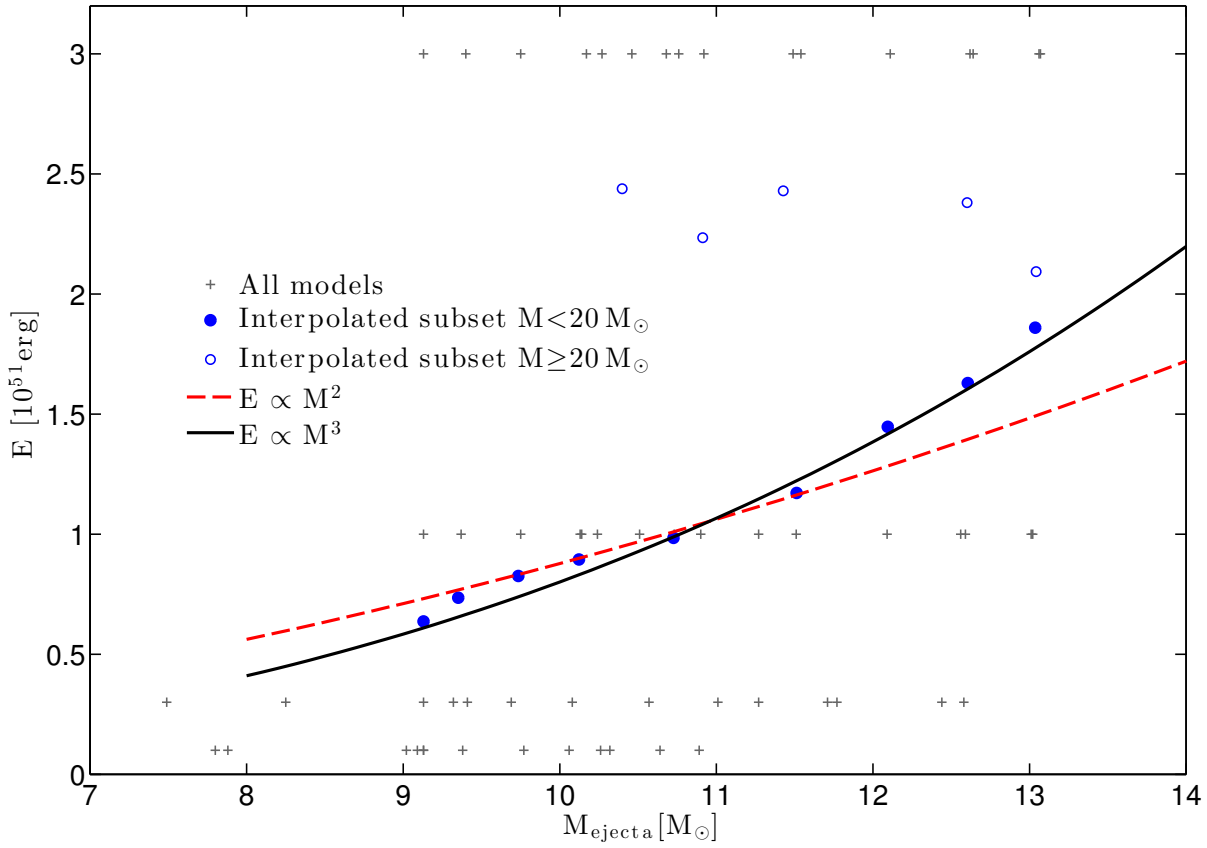

Fig. S3. Same as Figure S2, replacing initial masses with ejecta masses. The correlation now is closer to $E \propto M^3$, but breaks at large mass, as mass loss becomes highly non-linear.

Table 1.

SN name	M ($M_\odot$)	Source
1999an	< 18	(*2*)
1999br	< 15	(*2*)
1999em	< 15	(*2*)
1999gi	< 14	(*2*)
2001du	< 15	(*2*)
2002hh	< 18	(*2*)
2003gd	8^{+2}_{-2}	(*4*)
2003ie	< 25	(*2*)
2004A	12^{+2}_{-2}	(*4*)
2004am	12^{+7}_{-3}	(*2*)
2004dg	< 12	(*2*)
2004dj	15^{+3}_{-3}	(*2*)
2004et	11^{+2}_{-1}	(*10*)
2005cs	10^{+3}_{-2}	(*4*)
2006bc	< 12	(*2*)
2006my	10^{+2}_{-2}	(*4*)
2006ov	< 11	(*2*)
2007aa	< 12	(*2*)
2008bk	9^{+4}_{-1}	(*2*)
2009kr	21^{+3}_{-3}	(*5*)
2009md	8^{+6}_{-1}	(*2*)
2012aw	18^{+2}_{-2}	(*7*)
2012ec	18^{+4}_{-4}	(*9*)

Table S1: Progenitor Sample

Table 2.

SN name	cz_{CMB} (km s^{-1})	Explosion date	$v_{Fe\,II}$(50d) (km s^{-1})	Number of spectra	Source
1999br	960	–	1550 ± 300	–	(*19*)
1999em	717	25/10/1999 ± 4	3450 ± 80	28	(*31*)
1999gi	592	7/12/1999 ± 4	3680 ± 120	15	(*32*)
2002hh	40	29/10/2002 ± 2	4320 ± 400	6	(*33*)
2003gd	657	18/ 3/2003 ± 21	2930 ± 230	4	(*34*)
2004A	852	6/ 1/2004 ± 3	3410 ± 180	1	(*35*)
2004dj	133	30/ 6/2004 ± 10	3080 ± 130	5	(*36*)
2004et	40	23/ 9/2004 ± 0	3940 ± 110	12	(*37*)
2005cs	463	28/ 6/2005 ± 1	2160 ± 130	7	(*38*)
2006my	788	28/ 8/2006 ± 10	2590 ± 180	3	(*39, 40*)
2006ov	1566	7/ 9/2006 ± 10	2040 ± 200	6	(*39, 40*)
2007aa	1465	19/ 1/2007 ± 10	2940 ± 120	4	(*40*)
2008bk	230	25/ 3/2008 ± 2	1970 ± 90	2	(*41*)
2009kr	1939	28/10/2009 ± 10	4960 ± 280	8	(*5*)
2009md	1308	27/11/2009 ± 8	2290 ± 240	4	(*42*)
2012aw	778	16/ 3/2012 ± 1	4040 ± 90	9	(*7*)
2012ec	1408	7/ 8/2012 ± 5	3890 ± 410	4	(*9*)

Table S2: Spectroscopy

References and Notes

1. S. J. Smartt, J. J. Eldridge, R. M. Crockett, J. R. Maund, *MNRAS* **395**, 1409 (2009).

2. M. Fraser, *et al.*, *MNRAS* **417**, 1417 (2011).

3. R. M. Crockett, *et al.*, *MNRAS* **410**, 2767 (2011).

4. J. Maund, E. Reilly, S. Mattila, *ArXiv: 1302.7152* (2013).

5. N. Elias-Rosa, *et al.*, *ApJL* **714**, L254 (2010).

6. M. Fraser, *et al.*, *ApJL* **714**, L280 (2010).

7. S. D. Van Dyk, *et al.*, *ApJ* **756**, 131 (2012).

8. M. Fraser, *et al.*, *ApJL* **759**, L13 (2012).

9. J. R. Maund, *et al.*, *MNRAS* **431**, L102 (2013).

10. A. Jerkstrand, *et al.*, *A&A* **546**, A28 (2012).

11. S.-C. Yoon, M. Cantiello, *ApJL* **717**, L62 (2010).

12. R. Barbon, F. Ciatti, L. Rosino, *A&A* **72**, 287 (1979).

13. D. Poznanski, *et al.*, *PASP* **114**, 833 (2002).

14. A. V. Filippenko, *ARA&A* **35**, 309 (1997).

15. D. Poznanski, *et al.*, *ApJ* **694**, 1067 (2009).

16. W. Li, *et al.*, *MNRAS* **412**, 1441 (2011).

17. I. Arcavi, *et al.*, *ApJL* **756**, L30 (2012).

18. E. M. Schlegel, *AJ* **111**, 1660 (1996).

19. M. Hamuy, P. A. Pinto, *ApJ* **566**, L63 (2002).

20. P. Nugent, *et al.*, *ApJ* **645**, 841 (2006).

21. D. Poznanski, P. E. Nugent, A. V. Filippenko, *ApJ* **721**, 956 (2010).

22. L. Dessart, D. J. Hillier, *A&A* **439**, 671 (2005).

23. D. Kasen, S. E. Woosley, *ApJ* **703**, 2205 (2009).

24. O. Yaron, A. Gal-Yam, *PASP* **124**, 668 (2012).

25. J. M. Silverman, *et al.*, *MNRAS* **425**, 1789 (2012).

26. S. Blondin, J. L. Tonry, *ApJ* **666**, 1024 (2007).

27. G. J. Babu, E. D. Feigelson, *Communications in Statistics-Simulation and Computation* **21**, 533 (1992).

28. M. G. Akritas, M. A. Bershady, *ApJ* **470**, 706 (1996).

29. S. Tremaine, *et al.*, *ApJ* **574**, 740 (2002).

30. L. Dessart, E. Livne, R. Waldman, *MNRAS* **408**, 827 (2010).

31. D. C. Leonard, *et al.*, *PASP* **114**, 35 (2002).

32. D. C. Leonard, *et al.*, *AJ* **124**, 2490 (2002).

33. M. Pozzo, *et al.*, *MNRAS* **368**, 1169 (2006).

34. S. D. Van Dyk, W. Li, A. V. Filippenko, *PASP* **115**, 1289 (2003).

35. M. A. Hendry, *et al.*, *MNRAS* **369**, 1303 (2006).

36. D. C. Leonard, *et al.*, *Nature* **440**, 505 (2006).

37. W. Li, S. D. Van Dyk, A. V. Filippenko, J.-C. Cuillandre, *PASP* **117**, 121 (2005).

38. W. Li, *et al.*, *ApJ* **641**, 1060 (2006).

39. W. Li, *et al.*, *ApJ* **661**, 1013 (2007).

40. R. Chornock, A. V. Filippenko, W. Li, J. M. Silverman, *ApJ* **713**, 1363 (2010).

41. S. D. Van Dyk, *et al.*, *AJ* **143**, 19 (2012).

42. T. N. Steele, M. T. Kandrashoff, A. V. Filippenko, *Central Bureau Electronic Telegrams* **2070**, 1 (2009).